UNITED STATES DEPARTMENT OF THE INTERIOR

GEOLOGICAL SURVEY

# Seismicity of the Livermore Valley, California Region 1969-1979

by

W. L. Ellsworth

S. M. Marks

Open file Report 80-515

Summary

Seismicity of the Livermore Valley, California, region for the 11-year period from 1969 through 1979 reveals a complex pattern of seismic strain energy release. Earthquake epicenters and focal mechanism solutions confirm the presence of numerous active faults in the region, all of which move in response to the regional stress field. A systematic evaluation of the relationship between the seismicity for this period and candidate faults leads to the classification of the Calaveras-Sunol, Concord, Greenville and Hayward faults as active faults. The Las Positas, Pleasanton and Verona faults are identified as probably active faults. The Livermore fault and the segment of the Williams fault located to the south of the Las Positas and Verona faults are classified as possibly active. However, a northern prolongation of the Williams fault said to exist to the north of the Las Positas and Verona faults is unsupported by seismological evidence. Additionally, the connection between the Livermore fault and northwest trending fault said to exist to the south of the Las Positas fault is also unsupported by seismological evidence.

Earthquake focal mechanism solutions for events near Vallecitos Valley demonstrate that this region is a zone of active thrust faulting. Available seismological data indicates that some of these thrust faulting events are in probable association with the Verona fault. Better microearthquake instrumental coverage and improved knowledge of crustal structure in the Vallecitos-Livermore area should allow this relationship to be demonstrated.

## Introduction

The Livermore Valley of central California, approximately 60 km east of San Francisco, is an east-west trending valley located between the northern end of the exposed Franciscan core of the Diablo Range to the south and the Mount Diablo diapir to the north. The region lies within the eastern third of the 100 km broad zone of active faulting and seismicity which comprises the San Andreas fault system in the San Francisco Bay region (Figures 1 and 2). Earlier studies (Lee et al., 1971; Bolt and Miller, 1975) of the seismicity of this region indicate a highly complex and spatially diffuse pattern of strain release. East of the Hayward fault this activity is poorly correlated with known faults. The absence of a clear correlation is, in part, a reflection of the volumetrically distributed nature of strain-release within the region. It is also related to the inadequacy of seismographic station coverage for most of the historical perod, and to an incomplete knowledge of crustal structure.

This report presents the results of a comprehensive and systematic re-analysis of the seismicity of the Livermore Valley region for the years 1969-1979. The basic earthquake phase data upon which this report is based comes from earthquake data collected and analyzed from records of the U.S.G.S. central California Microearthquake network. Within the Livermore region, this network of high-gain, short-period, vertical seismometers has an inter-station separation of 10 to 20 km (Figure 1, Table 1). Network instrumentation and analysis procedures are described in earthquake catalogs for the years 1969-1976 (Lee et al. 1972 a, b, and c; Wesson et al., 1972 a and b, 1973 a, 1974 a and b; Bufe et al., 1975; Lester *et al.*, 1976 a and b; Lester and Meagher, 1978; McHugh and Lester, 1978 a and b). Data from the period 1977-1979 are derived from earthquake catalogs that are in preparation.

The re-analysis of seismicity reported herein restricts its attention to the period for which microearthquake network coverage is adequate. Use of an improved crustal model significantly enhances the precision of the earthquake locations and improves the resolution of focal mechanism solutions. Over 3900 earthquakes from the period 1969-1979 have been relocated, and their hypocenter soutions have been reviewed for accuracy.

Table 1. Seismograph station coordinates, travel time delays in seconds and operation dates for stations used to locate earthquakes in the Livermore study area.

| STN | LAT | LON | ELEV | DELAY | OPERATION DATES |
|---|---|---|---|---|---|
| CAC | 37N 58.57 | 121W 45.62 | 74 | 0.61 | 731026 - PRESENT |
| CAI | 37N 51.63 | 122W 25.77 | 223 | -0.63 | 690808 - PRESENT |
| CAL | 37N 27.07 | 121W 47.95 | 265 | -0.11 | 671019 - PRESENT |
| CAO | 37N 20.96 | 121W 31.96 | 628 | -0.29 | 671019 - PRESENT |
| CBR | 37N 48.97 | 122W 3.72 | 610 | 0.01 | 690823 - PRESENT |
| CBW | 37N 55.45 | 122W 6.40 | 221 | -0.02 | 710428 - PRESENT |
| CCN | 37N 47.49 | 121W 56.89 | 219 | 0.37 | 760205 - PRESENT |
| CCO | 37N 15.46 | 121W 40.35 | 366 | 0.13 | 671013 - PRESENT |
| CCI | 37N 47.30 | 121W 57.00 | 185 | 0.45 | 700729 - 760205 |
| CCY | 37N 33.10 | 122W 5.45 | 67 | -0.37 | 750501 - PRESENT |
| CYH | 37N 33.54 | 122W 5.62 | 38 | -0.39 | 661215 - 750429 |
| CDO | 37N 43.80 | 121W 50.12 | 198 | 0.43 | 700729 - PRESENT |
| CDS | 37N 57.93 | 122W 15.17 | 109 | -0.27 | 731115 - PRESENT |
| CDU | 38N 1.78 | 122W 0.05 | 168 | 0.29 | 710428 - PRESENT |
| CLC | 37N 44.23 | 122W 3.83 | 312 | -0.02 | 721121 - PRESENT |
| CMC | 37N 46.88 | 122W 10.55 | 90 | -0.28 | 710720 - PRESENT |
| CMH | 37N 21.57 | 121W 45.38 | 518 | 0.02 | 690304 - PRESENT |
| CMJ | 37N 31.25 | 121W 52.23 | 498 | 0.04 | 720701 - PRESENT |
| CMO | 37N 43.68 | 121W 48.15 | 792 | 0.30 | 690417 - PRESENT |
| CMR | 37N 35.66 | 121W 38.22 | 500 | -0.02 | 690417 - PRESENT |
| CPL | 37N 37.88 | 121W 57.37 | 463 | 0.00 | 690627 - PRESENT |
| CRA | 37N 46.03 | 121W 56.25 | 171 | 0.24 | 760902 - PRESENT |
| CRP | 37N 54.75 | 121W 54.33 | 331 | -0.15 | 700918 - PRESENT* |
| CSC | 37N 17.11 | 121W 46.35 | 128 | 0.43 | 670610 - PRESENT |
| CSH | 37N 38.88 | 122W 2.57 | 170 | -0.10 | - PRESENT/ |
| CTL | 37N 39.44 | 121W 38.63 | 458 | 0.23 | 770623 - PRESENT |
| CRK | 37N 14.50 | 122W 7.82 | 607 | -0.07 | 731101 - 760911 |
| MDC | 37N 52.90 | 121W 54.85 | 117 | -0.15 | 670527 - 740601 |
| MDO | 37N 52.04 | 121W 55.69 | 719 | -0.15 | 700527 - 700729 |
| MHC | 37N 20.50 | 121W 38.50 | 1282 | -0.25 | 1887 - PRESENT |
| JAL | 37N 9.50 | 121W 50.82 | 244 | -0.22 | 681016 - PRESENT |
| JBC | 37N 9.62 | 122W 1.57 | 660 | -0.03 | 690521 - PRESENT |
| JMG | 37N 38.22 | 122W 28.43 | 201 | -0.65 | 710831 - PRESENT |
| JPR | 37N 47.70 | 122W 28.43 | 107 | -0.46 | 760406 - PRESENT |
| JSA | 37N 34.95 | 122W 25.03 | 207 | -0.49 | - PRESENT/ |
| JSC | 37N 17.07 | 122W 7.42 | 357 | -0.22 | 661223 - PRESENT |
| JSF | 37N 24.31 | 122W 10.55 | 143 | -0.21 | 661213 - PRESENT |
| JSG | 37N 16.96 | 122W 3.00 | 198 | 0.28 | 750122 - PRESENT |
| JSJ | 37N 20.03 | 122W 5.48 | 122 | 0.13 | 661223 - PRESENT |
| JSS | 37N 10.17 | 121W 55.84 | 946 | -0.13 | 750122 - PRESENT |
| JST | 37N 12.41 | 121W 47.84 | 149 | -0.15 | 751002 - PRESENT |
| JWS | 37N 25.08 | 122W 16.33 | 280 | -0.24 | 661221 - PRESENT |
| NHM | 38N 9.28 | 121W 48.02 | 65 | 0.76 | 710429 - PRESENT |

* Station was intermittent during this time period.
/ No installation date available.

Analysis Procedure

Routine earthquake locations reported in the U.S.G.S. catalogs for central California for the period 1969-1979 were determined using a simple crustal model (Wesson, et al., 1972a). Owing to the diverse assemblage of geologic provinces within the area spanned by the network, this model necessarily represents a simplistic first attempt at characterizing the average velocity structure of the region. Detailed studies of crustal structure demonstrate that while this model produces acceptable earthquake locations for many purposes, it fails to provide locations as accurate and precise as can be obtained from the same arrival time data using localized structural models (Mayer-Rosa, 1973). Consequently, we have developed a velocity model appropriate for sources in the Livermore region and have used that model to systematically relocate all events detected by the U.S.G.S. network during 1969-1979.

This model is specified by a sequence of homogeneous, plane, horizontal layers overlying a half-space. The velocity within each layer is derived from explosion and earthquake travel time data using a least-squares adjustment procedure developed by Crosson (1976) and Aki and Lee (1976). A total of 1494 P-wave observations for 9 explosions and 57 earthquakes were inverted to determine the veocity model given in Table 2. This model is very similar to previous models for the Diablo Range (Byerly, 1939; Stewart, 1968) in that its most important feature is a shallow crustal refractor with a P-wave velocity between 5.6 and 5.7 km/s. The principal refinement of the model in Table 2 is the improved resolution of the average vertical velocity gradient in the seismogenic part of the crust (2-12 km). The velocity of 6.8 km/s adopted for the half-space below 13 km depth, although not well-constrained by the data, is consistent with both of the earlier studies.

Structural details near the surface cannot be adequately resolved by the available data. Because of the relative importance of near-surface structural features in the earthquake location problem, a set of station travel time adjustments (Table 1) was developed using the same procedure employed to determine the velocity structure.

Comparisons between earthquake locations routinely reported by U.S.G.S. and those obtained with the model described above show that the new model greatly improves the relative precision of the locations. Use of this model typically reduces the residual travel time variance by 50 to 75%. Systematic differences in epicentral locations generally show the relocations to define narrower zones of seismicity, especially along the Calaveras and Hayward faults. However, the sytematic displacement of the epicenters from these faults (Figure 3) strongly suggest that the locations may contain a systematic biase of 1 km or more.

A small calibration explosion located near San Ramon (Figure 1) provides an independent data set for evaluating the absolute precision of the models. Relocation of this event using the refined crustal structure gives a surface focus epicenter located 770 m north-northwest of the true shotpoint which is within the 95% confidence ellipse of the epicenter. Relocation of the shot using the standard crustal structure gives a location 1.5 km NW of the shotpoint, which lies outside of the 95% confidence interval.

Table 2. Crustal velocity structure of the Livermore region determined from joint inversion of explosion and earthquake travel time data.

| Velocity (km/s) | Depth to top layer (km) |
|---|---|
| 3.4 | 0.0 |
| 4.7 | 1.0 |
| 5.2 | 3.0 |
| 5.6 | 5.0 |
| 5.7 | 7.0 |
| 5.8 | 9.0 |
| 6.0 | 11.0 |
| 6.8 | 13.0 |

## Earthquake Locations in the Livermore Region

Relocated epicenters for earthquakes in the greater Livermore region confirm a complex pattern of seismic strain energy release in the northern Diablo Range (Figure 3). Seismic activity within the region is sharply bounded on the southwest by the nearly continuous zone of seismicity aligned along the Hayward and Calaveras-Sunol faults. Its eastern boundary is diffuse in character and approximately corresponds to the western edge of the San Joaquin Valley. Earthquake focal depths within the study area extend from near the surface to over 15 km depth, the normal range of focal depths in central California (Wesson et al., 1973b).

Between the Hayward fault and the San Joaquin Valley, earthquake epicenters form randomly distributed clusters which do not display an obvious systematic relationship to mapped faults. The densest concentration of activity in this zone lies 10 km south of Mount Diablo near the town of Danville (Figure 2). This focal volume has been the site of recurrent swarm activity since at least 1970 (Lee et al, 1971). To the north of this swarm area, epicenters concentrate within a 10 km broad zone lying between the Calaveras-Sunol and Concord faults. Along the Calaveras-Sunol fault and within the Livermore Valley a markedly lower level of seismicity can be seen in this 11 year sample. South of the Livermore Valley, within the north end of the Diablo Range, earthquake epicenters define several tight clusters imbedded in a diffuse background of activity.

The two faults in the region which are clearly defined by earthquake epicenters are the Hayward and Calaveras-Sunol faults (Figure 3). The breadth of the epicenteral distribution measured transverse to the strike of these faults varies substantially with position along the fault. Locally the width exceeds 3 km, or 6 times the average relative epicentral error. We conclude that seismicity associated with these two vertical strike slip faults has a resolvable breadth which locally prevents unique association of the seismicity with a single fault trace. To the east of these seismically well-defined faults, the distributed nature of the seismicity complicates the association of specific earthquakes with known faults.

Selected focal mechanism solutions (Figure 4) illustrate the predominance of strike slip faulting within the region. Focal mechanisms along the Hayward and Calaveras faults show that these faults form a continuous northwest-trending dextrel shear zone. To the east of these faults, the dextrel slip plane for most focal mechanism is rotated clockwise from northwest to north. This pattern is similar to that observed in the Bear Valley region, southeast of Hollister, California along the San Andreas and Calaveras-Paicines faults (Ellsworth, 1975). Note also the presence of some thrust fault solutions , near Danville, Livermore, and Vallecitos Valley (Figure 4).

A summary diagram of P and T axes from available mechanism data (Figure 5) indicates that seismic strain energy release occurs predominantly on nearly vertical planes in response to a shear stress field oriented roughly parallel to the principal faults of the region.

These data are also in good agreement with the geodetically measured north-south compressional and east-west extensional strain field. (Savage and Burford, 1973; Thatcher, 1975). Within the region northeast of the Hayward and Calaveras faults, focal mechanism solutions show a continuous progression from strike slip to thrust faulting. Normal faulting cannot be documented anywhere in the region on the basis of available first motion data.

## Classification of Fault Activity Using Seismological Evidence

Documentation of the active or inactive state of a specific fault from a limited record of seismicity data, such as is available for the Livermore region, is not a symmetrically posed question. While it is possible to demonstrate unambiguously the active state of a specific fault through the geometric relationship of earthquake hypocenters and focal mechanism solutions to the surface expression of the fault, the inactive state (or non-existence) of candidate faults cannot be conclusively demonstrated from these data. The absence of correlative seismicity by itself, is not evidence for a specific fault being in an inactive state. For example, sections of the San Andreas fault which ruptured in great earthquakes in 1857 and 1906, are presently seismically quiet. The presence of a well documented regional stress field of known orientation requires that all faults whose movement could be compatable with the stress field be considered as potentially active, unless specific geologic data indicate otherwise.

Quantitative evaluation of low levels of seismicity as indicators of potential activity of a fault is also not possible at present, given our limited understanding of the earthquake process. The specific example of the Greenville fault is particularly poignant in this regard. Seismological evidence for the existence of the Greenville fault as an important component of the neotectonic framework of the region is comparatively weak on the basis of data shown in Figures 3 and 4. Yet this fault produced one of the largest earthquakes to strike the San Francisco Bay Region in this century on January 24, 1980 (Figure 6; Bonilla *et al.*, 1980). Clearly, even a very low level of seismicity in association with a specific fault is as important an indicator of fault activity as a dense alignment of epicenters along it.

In view of our incomplete knowledge of either the seismic record, the physical elements of the fault system or the physics of earthquakes themselves, what then can be learned from a comparison of seismicity data with a suite of potentially active faults? At best, we can state that a fault is active or probably active, but we cannot quantify either the likelihood of occurence of its maximum earthquake or the magnitude of that event. The answer to these questions presently comes from the geologic record as aided by the historic record of large earthquakes, where available.

However, within these limitations, the systematic use of seismicity data for classification of fault activity requires a consistent set of rules. Table 3 lists the seismological criteria adopted here to define four broad classifications of fault activity. The specific names applied to the classifications are understood to derive meaning from these criteria alone. In applying these rules to the problem at hand it is also understood that the term hypocenter encompasses not only the single best estimate of the earthquakes focus derived from the location procedure, but also the confidence region for that location.

Table 3. Fault Activity Classification Criteria From Seismicity Data

1. Seismically Active Fault: Presence of earthquake hypocenters on the geologically defined or inferred fault plane that have well-constrained focal mechanism solutions in agreement with movement on the fault plane. The correlation between earthquake hypocenters and the fault plane solutions must exclude, at a high confidence level, the association of those events with other candidate faults.
2. Probably Seismically Active Fault: Earthquake hypocenters located on the geologically inferred fault plane, the probable compatability of focal mechanism solutions with movement on the fault, and the existence of a regional stress field compatible with the geologic record fault movement. The correlation between earthquake hypocenters and the fault plane must be the most probable association. The possible association of the events with other faults may be permitted by the data.
3. Possibly Seismically Active Fault: Earthquake hypocenters in possible association with the fault plane and the existence of a regional stress field compatible with the geologic record fault movement. Available first-motion data must agree with movement on the fault. The association between earthquake hypocenters and the fault plane permits the interpretation that they are related but it lacks the precision to demonstrate the correlation with reasonable confidence.
4. Fault Unsupported by Seismological Evidence: Absence of any seismological evidence in direct support of the existence of a proposed fault. Regional stress field may or may not agree with movement on the fault.

## Active Faults in the Livermore Region

The fault classification criteria given in Table 3 are applied on a fault by fault basis to candidate active faults of the Livermore region. The list of faults considered includes the principal recently active faults identified by Herd (Herd, 1977; Herd and Brabb, unpubl. admin. report, 1980, Figure 40), the Livermore fault (California Report Water Resources, 1963) and the Williams faults (Hall, 1958). Except where noted, seismicity data used in the classification of these faults is restricted to the 1969-1979 sample (Figures 3 and 4).

Calaveras-Sunol Fault: Seismically Active. This fault is clearly defined by a continuous, narrow zone of seismicity from the southern border of the study area to Calaveras Reservoir. Although the seismicity is systematically offset 0.5 km to the northeast of the mapped surface trace of the fault, the offset is smaller than the absolute uncertainty of the locations. We believe that it is an artifact of the location procedure caused by insufficiently detailed knowledge of crustal structure (Ellsworth and Moths, 1979). Well constrained focal mechanisms uniformly agree with right lateral movement on the fault. North of Calaveras reservoir, the Calaveras-Sunol fault is poorly defined by seismicity. There are a number of events in possible association with the fault plane, including several with strike slip focal mechanisms suitably oriented for right lateral slip on the fault. However, this correlation is not unique and may be fortuitous. The segment of this fault opposite Danville ruptured in the M 6 earthquake of 1861 (Toppozada, et al. 1979).

Concord Fault: Seismically Active. Seismicity associated with this fault forms the northeastern boundary of a diffuse zone of epicenters lying between the Concord and Calaveras-Sunol faults. Focal mechanism solutions indicate right-lateral movement on the fault.

Greenville Fault: Seismically Active. The location of this fault on the periphery of the network causes a degradation in the quality of epicentral determinations. This complicates the correlation of earthquakes with the mapped fault trace. It is clear, however, that this area is characterized by a lower level of activity than the Hayward, Calaveras-Sunol or Concord faults. Several strong earthquakes locate near the fault (including the 21 June 1977 M 4.7 event at 37° 38'N lat., 121° 40'W long.) and have focal mechanism solutions compatable with right slip on the fault. A careful re-examination of earthquake locations in the vicinity of the 24 January 1980 M 5.8 earthquake, shows that some earthquakes from the period 1969-1979 occurred within the aftershock volume of the 1980 earthquake. This event ruptured strands of the fault mapped by Herd (1977) and triggered seismic activity along a 30-km portion of the fault (Figure 6). Had the January 1980 earthquake sequence not occurred, or if its relationship to the Greenville fault been unclear, the criteria of Table 3 would have led to classification of this fault as being probably active.

Hayward Fault: Seismically Active. This fault produced large earthquakes in 1836 and 1868 (Lawson and others, 1908; Toppozada et al., 1979). It is currently creeping at an average rate of about 1/2 cm/yr (Nason, 1971) and is well-defined by its seismicity. Focal mechanism solutions clearly indicate right lateral strike slip motion. The continuous zone of seismicity connecting the Hayward fault to the Calaveras fault at Calaveras reservoir follows the trace of the Mission fault of Hill (1958).

Las Positas fault: Probably Seismically Active. This northeast-southwest trending left lateral strike slip fault has a unique orientation among active faults in the San Francisco Bay Region (Herd, 1979; Herd and Brabb, unpubl. admin. report, 1980). It is conjugate to the Greenville and Calveras-Sunol faults and thus responds to the same stress field known to be acting on them. Some earthquake epicenters in Figure 3 appear to be associated with this fault. First motion data for these events are consistent with left lateral slip on a vertical plane parallel to the strike of the Las Positas fault. However, they are not sufficiently well constrained to unambiguously demonstrate activity.

Livermore Fault: Possibly Seismically Active. Some of the many scattered epicenters within the Livermore Valley locate near the trace of the Livermore fault, a northwest-trending fault inferred to exist near Livermore (Calif. Dept. of Water Resources, 1963). Focal mechanism solutions for these events are inconsistent with movement on this fault.

Strike slip focal mechanisms indicate movement on fault planes at an angle of about $45^{\circ}$ to the Livermore fault. Thrust solutions correspond to events with foci that are too deep to be related to the fault. However, other poorly constrained focal mechanism solutions might possibly agree with dextral slip on the fault.

South of the Las Positas fault, a single focal mechanism would suggest right lateral motion on a fault proposed by Earth Science Associates (1979) to be the southern extension of this fault. However, this mechanism could equally reflect left-lateral movement on a fault that parallels the Las Positas fault at this point as mapped by Herd (1977). There is no seismological evidence which directly suggests a connection between the proposed pieces of the Livermore fault.

Furthermore, it is geometrically impossible for both the Las Positas and Livermore faults to exist as continuous features through their point of intersection. Geologic evidence strongly favor the interpretation of the Las Positas fault as the through-going fault (Herd, 1977).

Pleasanton Fault: Probably Seismically Active. Seismological evidence supports the identification of this fault as an active fault. However, few epicenters actually locate near and their association with the fault cannot be unambiguously demonstrated. The distribution of earthquake hypocenters and orientation of their focal mechanism to the north of the Pleasanton fault strongly suggest that this fault continues to the north along the east side of San Ramon Valley.

Verona Fault: Probably Seismically Active. Earthquake locations and focal mechanisms support the interpretation of this feature as a northeast dipping thrust fault. Focal mechanism solutions for events in probable association with the inferred downward continuation of the fault plane (Herd and Brabb, unpubl. admin. report, 1980) all agree with north over south thrusting on the fault plane. Relatively weak focal depth control caused by inadequate seismographic coverage prevents the unambiguous classification of this fault as active by the criteria of Table 3. Most of the events with epicenters within 1 km of the surface trace of the Verona fault are probably not associated with it, as they lie several kilometers below the inferred fault plane. We interpret these events to result from movement on as yet unidentified faults. However, some events located within 600 m of the fault have very shallow foci, and may be related to the Verona fault. This question is considered in greater detail in a following section of this report.

Northern Segment of the Williams Fault: Fault Unsupported by Seismological Evidence; Southern Segment of the Williams Fault: Possibly Seismically Active. Discussion of the Williams fault maybe logically divided between the segment of the fault said to exist north of the Las Positas and Verona faults (Earth Science Associates, 1979) and the segment south of them. Among the earthquakes in possible association with the northern segment of the Williams fault (Figure 3), all events with resolvable focal mechanism solutions can be demonstrated to be unrelated to it by virture of incompatable focal mechanisms (Figure 8).

Two of these events have thrust solutions which place them in probable association with the Verona fault. The third event has a strike slip mechanism with nodal planes oriented at approximately 45 to the Williams fault. The existence of this segment of the fault is thus unsupported by seismological evidence.

The southern segment of the Williams fault has numerous small earthquakes located near its trace. Nodal planes of focal mechanism solutions for events located near this segment of the Williams fault do not agree with the orientation of this fault. Other poorly constrained mechanisms may possibly agree with dextral slip on the fault. Seismicity within this region is widely scattered and does not define any single fault but requires faulting to be distributed on numerous faults.

## Seismicity Near the Verona Fault

The classification of faults in the Livermore region presented above identified the Verona fault as a probably seismically active fault. Because this fault is a thrust, the relationship of earthquakes to the fault cannot be readily inferred from the maps in Figures 3 and 4. Inferences about the association of specific events with the fault must consider the three-dimensional relationship of the earthquakes to the fault plane at depth. The basic data relevant to this discussion are the earthquake hypocenter solutions, their estimated uncertainties and their focal mechanism solutions (Table 4, Figures 7 and 8).

In general, the location of most epicenters, relative to their neighbors, are well constrained throughout the region. The relative uncertainty in their locations (listed in Table 4) are considered to be a good estimate of the relative epicentral precision. Absolute errors of 1 km are possible since the velocity structure of this area is not known in detail.

The precision of focal depth determinations varies considerably throughout the region shown in Figure 7 because of the absence of nearby seismographic station coverage. The epicentral distance to the nearest station varies from just under 7 km to over 15 km. As the presence of a station within a focal depth of the earthquake is critical to the accurate determination of focal depth, most of the depths listed in Table 4 are known with less certainty than their corresponding epicenters.

This is reflected, in part, in larger focal depth uncertainties. Events shallower than about 3 km have artificially small depth error estimates. Their true uncertainty probably exceeds 2 km.

Focal mechanism solutions appearing in Figure 8 represent single event mechanisms for which the type of faulting could be clearly established. In detail, the strike and dip of any given nodal plane may be uncertain by 10° or more, owing to inadequate sampling of the radiation pattern and/or incomplete knowledge of crustal structure. The only exception to the statement applies to events with focal depths less than 2 km. Uncertainties in their depths permits interpretation of their mechanisms as either reverse faulting or strike slip faulting. The strike slip mechanisms appropriate to these events appear in Figure 8. Reverse fault planes for these events dip at 45° to the northeast.

It is apparent from the distribution of hypocenters and focal mechanism solutions for earthquakes occurring near the Verona fault (Figures 7 and 8) that the seismicity is not restricted to a single fault plane. Focal mechanism solutions show a continuous progression from strike slip to thrust faulting, all under the influence of a north-northeast-south-southwest oriented compressive stress field. In cross-section (a-a', Figure 7; Figure 9) it can be seen that some of the events with thrust-type focal mechanisms locate near the inferred downward continuation of the Verona fault plane. The dip of the fault adopted in Figure 9 corresponds to the dip of the Verona fault where it is last seen in borehole BH-3 (Herd and Brabb, unpubl. admin. report, 1980, Figure 3). These events are in probable association with this fault. Although they are too few in number, and have sufficiently uncertain focal depths to prove this point, they demonstrate that thrust faulting, at depth, extends into the center of the Livermore Valley. Therefore, it is conceivable that the Verona fault extends to a depth of 6 km or more.

The occurrence of these and other thrust events (Figure 8) supports the tectonic framework for the Livermore Valley proposed by Herd and Brabb (unpubl. admin. report, 1980, Figure 41). Left-slip movement on the Las Positas fault compresses the region immediately north of its projected intersection with the Calaveras-Sunol fault. Right-slip movement on the Calaveras-Sunol fault north of this imaginary point of intersection similarly compresses this zone. Reverse movement on faults within the zone, including the Verona, serves to relieve these stresses.

Not all of the earthquakes within this zone have reverse faulting mechanisms. Several of the deeper events have strike slip fault plane solutions. The shear stress field of the greater region, inferred from regional focal mechanisms (Figure 5), must therefore be transmitted through this zone as well.

The shallow event located within 1 km of the surface trace of the Verona fault (Figure 7) may also posess a strike slip mechanism. This event, which occurred on September 10, 1970, and the event of October 6, 1970 have unusually shallow focal depths, probably less than 2 km. Uncertainties in ray take-off angles for these shallow events permit the interpretation that they are thrust faulting events and that they locate on the Verona fault. However, their first motion patterns are more readily explained by strike slip faulting.

Although the precise relationship of these events to the Verona fault is unknown, their tectonic significance is clear. Their presence at shallow depth near or within the Verona fault zone demonstrates that the tectonic stress locally exceeds the failure strength of the rock. The P-axes of the focal mechanism solutions for these events have a northeast-southwest orientation for either interpretation of their mechanisms. This orientation is favorable to the sense of displacement of the Verona fault reported by Herd and Brabb (unpubl. admin. report, 1980).

In summary, available seismological evidence demonstrates: 1) that the Verona fault has earthquakes in probable association with its fault plane that have focal mechanisms in agreement with north-over-south thrust movement on the fault, 2) that regional stress field determined from focal mechanism solutions agrees with the tectonic interpretation of the fault, and 3) that shear stresses locally exceed the strength of the crust within 2 km or less of the known surface trace of the Verona fault.

## Acknowledgements

We are grateful to Allan Lindh and Darrell Herd for their thorough technical review of this paper. Bob Morris, Bob Page, and Bob Wallace made several useful suggestions which we have incorporated in the text. We also Thank, Barbara Moths, Linda Shijo, and Virgie Barba for their assistance in preparing the report.

Table 4. Catalog of earthquakes in the Vallecitos Valley and Western Livermore Valley region for 1969-1979

VALLECITOS VALLEY AND WESTERN LIVERMORE VALLEY EARTHQUAKES

| | | | HR | MN | SEC | LAT N | LONG W | DEPTH | MAG | NO | GAP | DMIN | RMS | ERH | ERZ | Q | QUADRANGLE |
|---|---|---|---|---|---|---|---|---|---|---|---|---|---|---|---|---|---|
| 1969 | APR | 25 | 7 | 55 | 40.8 | 37-35.0 | 121-50.6 | 3.7 | 1.2 | 11 | 183 | 15.2 | 0.08 | 0.5 | 1.1 | C | LA COSTA VALLEY |
| 1970 | JAN | 26 | 23 | 30 | 19.9 | 37-35.3 | 121-50.4 | 4.0 | 1.1 | 9 | 125 | 11.3 | 0.07 | 0.4 | 0.8 | D | LA COSTA VALLEY |
| | APR | 17 | 3 | 17 | 53.9 | 37-36.7 | 121-46.1 | 0.3 | 0.5 | 6 | 182 | 11.8 | 0.02 | 0.2 | 1.3 | C | LA COSTA VALLEY |
| | JUN | 29 | 14 | 14 | 12.7 | 37-42.2 | 121-47.6 | 11.5 | 1.3 | 10 | 135 | 12.0 | 0.08 | 0.6 | 0.8 | D | LIVERMORE |
| | JUL | 2 | 6 | 38 | 43.4 | 37-42.4 | 121-46.9 | 13.0 | 1.8 | 12 | 143 | 11.7 | 0.07 | 0.5 | 1.1 | B | LIVERMORE |
| | | 2 | 7 | 1 | 20.5 | 37-42.4 | 121-46.8 | 12.9 | 1.6 | 12 | 144 | 11.8 | 0.07 | 0.4 | 0.3 | D | LIVERMORE |
| | | 2 | 8 | 4 | 55.5 | 37-42.4 | 121-47.0 | 12.8 | 1.9 | 14 | 142 | 11.7 | 0.07 | 0.5 | 0.4 | B | LIVERMORE |
| | | 2 | 8 | 46 | 58.5 | 37-42.5 | 121-47.1 | 12.8 | 1.3 | 12 | 142 | 11.6 | 0.08 | 0.5 | 0.4 | B | LIVERMORE |
| | SEP | 10 | 7 | 24 | 24.0 | 37-37.2 | 121-51.6 | 0.2 | 2.2 | 15 | 85 | 8.5 | 0.06 | 0.2 | 1.6 | D | LA COSTA VALLEY |
| | OCT | 6 | 10 | 7 | 14.5 | 37-37.7 | 121-51.2 | 0.6 | 1.8 | 7 | 96 | 9.0 | 0.06 | 0.3 | 2.9 | B | LIVERMORE |
| 1971 | APR | 23 | 12 | 9 | 23.0 | 37-36.1 | 121-54.1 | 4.4 | 0.8 | 9 | 92 | 5.8 | 0.07 | 0.4 | 0.7 | B | NILES |
| | JUN | 14 | 2 | 22 | 25.6 | 37-42.3 | 121-53.9 | 14.9 | 1.4 | 16 | 84 | 6.2 | 0.10 | 0.5 | 0.8 | A | DUBLIN |
| | | 29 | 15 | 1 | 50.6 | 37-35.3 | 121-54.6 | 9.4 | 1.5 | 15 | 106 | 6.3 | 0.07 | 0.3 | 0.5 | D | NILES |
| | JUL | 28 | 5 | 41 | 57.2 | 37-38.1 | 121-51.5 | 4.6 | 1.3 | 8 | 92 | 8.7 | 0.05 | 0.3 | 0.5 | B | LIVERMORE |
| | SEP | 12 | 1 | 2 | 29.4 | 37-36.5 | 121-47.0 | 1.4 | 1.5 | 9 | 115 | 13.0 | 0.07 | 0.6 | 1.1 | B | LA COSTA VALLEY |
| | OCT | 18 | 14 | 36 | 59.5 | 37-36.8 | 121-47.1 | 1.5 | 1.2 | 7 | 118 | 13.2 | 0.04 | 0.4 | 0.6 | B | LA COSTA VALLEY |
| | NOV | 22 | 3 | 16 | 23.6 | 37-36.7 | 121-45.7 | 8.4 | 1.9 | 10 | 126 | 11.2 | 0.04 | 0.4 | 0.9 | D | LA COSTA VALLEY |
| | DEC | 4 | 13 | 31 | 34.5 | 37-41.9 | 121-49.1 | 11.9 | 1.0 | 10 | 119 | 3.9 | 0.09 | 0.6 | 0.8 | B | LIVERMORE |
| | | 5 | 4 | 40 | 45.5 | 37-42.2 | 121-48.8 | 12.9 | 1.3 | 10 | 123 | 3.5 | 0.09 | 0.7 | 0.4 | B | LIVERMORE |
| 1972 | JAN | 2 | 12 | 12 | 4.5 | 37-42.3 | 121-54.2 | 6.8 | 1.1 | 7 | 110 | 6.6 | 0.08 | 0.7 | 1.1 | B | DUBLIN |
| | FEB | 14 | 4 | 45 | 55.2 | 37-37.4 | 121-48.3 | 0.8 | 0.3 | 8 | 114 | 12.2 | 0.08 | 0.5 | 3.7 | C | LA COSTA VALLEY |
| | JUL | 9 | 22 | 15 | 40.4 | 37-40.6 | 121-46.3 | 4.4 | 1.9 | 9 | 138 | 8.1 | 0.11 | 0.9 | 1.5 | B | LIVERMORE |
| | AUG | 2 | 21 | 29 | 0.6 | 37-36.6 | 121-53.9 | 5.4 | 1.4 | 12 | 73 | 5.7 | 0.08 | 0.4 | 1.0 | B | NILES |
| | | 25 | 16 | 26 | 45.9 | 37-36.9 | 121-50.2 | 11.6 | 0.9 | 8 | 96 | 10.6 | 0.05 | 0.4 | 0.5 | D | LA COSTA VALLEY |
| | OCT | 3 | 2 | 8 | 2.4 | 37-36.8 | 121-53.9 | 6.4 | 1.7 | 18 | 72 | 5.4 | 0.06 | 0.2 | 0.4 | A | NILES |
| | | 17 | 2 | 32 | 4.0 | 37-39.8 | 121-50.5 | 1.5 | 1.7 | 10 | 101 | 7.3 | 0.11 | 0.5 | 0.9 | B | LIVERMORE |
| | DEC | 16 | 20 | 10 | 1.1 | 37-38.4 | 121-45.1 | 0.1 | 1.8 | 10 | 131 | 11.3 | 0.09 | 0.5 | 2.6 | C | LIVERMORE |
| 1973 | JAN | 1 | 7 | 24 | 43.9 | 37-38.1 | 121-51.2 | 2.5 | 0.7 | 8 | 94 | 9.0 | 0.04 | 0.3 | 0.5 | D | LIVERMORE |
| | | 5 | 16 | 56 | 57.7 | 37-37.5 | 121-54.0 | 6.4 | 1.7 | 17 | 72 | 5.0 | 0.06 | 0.2 | 0.4 | A | NILES |
| | | 15 | 23 | 12 | 38.1 | 37-38.5 | 121-52.9 | 10.1 | 0.8 | 8 | 81 | 6.7 | 0.04 | 0.3 | 0.7 | A | DUBLIN |
| | MAR | 2 | 8 | 46 | 32.4 | 37-36.1 | 121-46.5 | 2.1 | 0.5 | 6 | 116 | 12.1 | 0.05 | 0.4 | 0.8 | B | LA COSTA VALLEY |
| | | 14 | 10 | 55 | 20.3 | 37-35.4 | 121-50.5 | 8.5 | 0.5 | 8 | 138 | 8.0 | 0.07 | 0.5 | 1.2 | B | LA COSTA VALLEY |
| | | 16 | 9 | 42 | 40.4 | 37-35.3 | 121-50.1 | 7.4 | 0.4 | 7 | 88 | 8.2 | 0.07 | 0.5 | 1.5 | B | LA COSTA VALLEY |
| | APR | 5 | 13 | 31 | 26.3 | 37-35.3 | 121-54.3 | 9.2 | 1.1 | 10 | 76 | 6.5 | 0.05 | 0.3 | 0.5 | A | NILES |
| | | 11 | 4 | 6 | 43.0 | 37-35.3 | 121-54.2 | 8.3 | 0.4 | 8 | 71 | 6.6 | 0.08 | 0.5 | 1.0 | A | NILES |
| | | 18 | 19 | 36 | 58.2 | 37-36.5 | 121-46.0 | 6.8 | 1.8 | 13 | 105 | 11.5 | 0.09 | 0.4 | 0.8 | B | LA COSTA VALLEY |
| | JUN | 1 | 11 | 42 | 13.6 | 37-38.6 | 121-49.5 | 4.1 | 1.4 | 11 | 102 | 9.6 | 0.05 | 0.2 | 0.4 | B | LIVERMORE |
| | AUG | 17 | 13 | 47 | 52.7 | 37-40.3 | 121-47.5 | 6.4 | 1.6 | 15 | 126 | 7.5 | 0.10 | 0.5 | 0.9 | D | LIVERMORE |
| | OCT | 29 | 9 | 49 | 50.2 | 37-37.6 | 121-53.7 | 6.7 | 0.5 | 10 | 75 | 5.4 | 0.03 | 0.2 | 0.3 | A | DUBLIN |
| | NOV | 27 | 10 | 54 | 46.5 | 37-35.3 | 121-48.5 | 6.5 | 0.5 | 7 | 96 | 9.3 | 0.06 | 0.4 | 1.9 | B | LA COSTA VALLEY |
| | | 28 | 8 | 51 | 51.1 | 37-36.1 | 121-54.4 | 8.0 | 0.6 | 8 | 94 | 5.5 | 0.08 | 0.6 | 1.1 | B | NILES |
| 1974 | FEB | 7 | 9 | 27 | 42.4 | 37-40.3 | 121-47.6 | 6.2 | 0.9 | 10 | 125 | 7.4 | 0.08 | 0.5 | 1.4 | B | LIVERMORE |
| | | 26 | 15 | 54 | 5.9 | 37-41.4 | 121-49.1 | 8.6 | 1.1 | 12 | 141 | 4.7 | 0.07 | 0.4 | 0.4 | D | LIVERMORE |
| | MAR | 18 | 17 | 49 | 27.2 | 37-37.6 | 121-45.6 | 5.5 | 1.5 | 7 | 138 | 11.4 | 0.05 | 0.6 | 7.1 | C | LIVERMORE |
| | | 21 | 2 | 34 | 45.0 | 37-35.2 | 121-49.3 | 7.7 | 1.0 | 9 | 91 | 8.4 | 0.04 | 0.2 | 0.6 | D | LA COSTA VALLEY |
| | APR | 10 | 5 | 59 | 45.2 | 37-39.7 | 121-47.8 | 4.5 | 0.5 | 6 | 142 | 8.3 | 0.04 | 0.2 | 0.4 | B | LIVERMORE |
| | SEP | 29 | 22 | 20 | 4.6 | 37-36.7 | 121-46.5 | 5.0 | 1.5 | 11 | 121 | 12.3 | 0.11 | 0.5 | | C | LA COSTA VALLEY |
| | | 29 | 22 | 22 | 12.5 | 37-36.6 | 121-46.6 | 7.4 | 0.9 | 6 | 119 | 12.5 | 0.02 | 0.2 | 1.3 | B | LA COSTA VALLEY |
| | OCT | 20 | 3 | 33 | 34.0 | 37-41.6 | 121-47.2 | 10.0 | 1.7 | 17 | 125 | 5.9 | 0.05 | 0.2 | 0.3 | B | LIVERMORE |
| | | 20 | 3 | 44 | 12.3 | 37-42.0 | 121-46.7 | 11.1 | 1.0 | 10 | 143 | 6.1 | 0.10 | 0.7 | 1.0 | B | LIVERMORE |
| | | 20 | 3 | 44 | 44.8 | 37-41.8 | 121-47.2 | 10.1 | 1.9 | 22 | 126 | 5.7 | 0.09 | 0.3 | 0.3 | B | LIVERMORE |
| | | 20 | 5 | 6 | 29.9 | 37-41.6 | 121-46.9 | 9.8 | 1.9 | 19 | 127 | 6.2 | 0.08 | 0.3 | 0.4 | D | LIVERMORE |
| | | 29 | 20 | 39 | 6.2 | 37-36.7 | 121-46.6 | 5.6 | 1.2 | 11 | 105 | 12.4 | 0.07 | 0.4 | 1.5 | B | LA COSTA VALLEY |
| | NOV | 23 | 10 | 29 | 53.3 | 37-35.4 | 121-47.6 | 2.1 | 0.9 | 7 | 101 | 10.3 | 0.03 | 0.2 | 0.4 | B | LA COSTA VALLEY |
| | | 24 | 4 | 29 | 0.7 | 37-35.4 | 121-47.6 | 2.4 | 1.1 | 10 | 101 | 10.2 | 0.06 | 0.3 | 0.6 | B | LA COSTA VALLEY |
| 1975 | FEB | 22 | 13 | 55 | 45.8 | 37-35.5 | 121-48.6 | 6.1 | 1.1 | 10 | 97 | 9.5 | 0.17 | 0.7 | 5.7 | B | LA COSTA VALLEY |
| | APR | 2 | 19 | 45 | 45.4 | 37-39.2 | 121-47.1 | 6.0 | 1.7 | 19 | 121 | 9.6 | 0.11 | 0.4 | 0.9 | B | LIVERMORE |
| | MAY | 25 | 13 | 34 | 57.6 | 37-36.5 | 121-46.7 | 6.6 | 2.1 | 23 | 105 | 12.6 | 0.05 | 0.2 | 0.3 | B | LA COSTA VALLEY |
| | JUL | 3 | 21 | 25 | 13.5 | 37-36.9 | 121-51.8 | 5.9 | 1.6 | 19 | 85 | 8.3 | 0.07 | 0.2 | 0.5 | B | LA COSTA VALLEY |
| | | 16 | 2 | 18 | 44.8 | 37-35.1 | 121-49.2 | 7.4 | 1.4 | 18 | 91 | 8.4 | 0.09 | 0.3 | 0.7 | B | LA COSTA VALLEY |
| | | 25 | 11 | 21 | 1.0 | 37-36.5 | 121-45.3 | 6.0 | 1.3 | 11 | 108 | 10.6 | 0.04 | 0.2 | 0.9 | D | LA COSTA VALLEY |
| | AUG | 14 | 19 | 5 | 30.3 | 37-37.9 | 121-51.4 | 5.8 | 2.0 | 21 | 89 | 8.8 | 0.07 | 0.2 | 0.5 | B | LIVERMORE |
| | | 18 | 1 | 43 | 22.1 | 37-38.1 | 121-51.4 | 5.1 | 1.3 | 14 | 89 | 8.8 | 0.08 | 0.3 | 2.4 | D | LIVERMORE |
| | NOV | 6 | 8 | 7 | 20.6 | 37-41.0 | 121-48.5 | 11.2 | 1.8 | 25 | 116 | 14.2 | 0.09 | 0.3 | 0.4 | B | LIVERMORE |
| | | 13 | 2 | 52 | 0.9 | 37-36.6 | 121-48.2 | 0.6 | 2.0 | 20 | 96 | 11.5 | 0.08 | 0.2 | 1.6 | B | LA COSTA VALLEY |
| | DEC | 25 | 20 | 9 | 36.4 | 37-37.2 | 121-47.4 | 6.6 | 1.2 | 13 | 104 | 12.9 | 0.07 | 0.3 | 1.0 | B | LA COSTA VALLEY |
| 1976 | JAN | 25 | 3 | 27 | 34.2 | 37-36.9 | 121-47.9 | 2.3 | 1.2 | 8 | 113 | 12.2 | 0.04 | 0.2 | 0.3 | D | LA COSTA VALLEY |
| | SEP | 4 | 22 | 48 | 55.0 | 37-38.2 | 121-46.1 | 0.4 | 1.5 | 6 | 142 | 11.9 | 0.05 | 0.4 | 3.0 | C | LIVERMORE |
| | | 5 | 2 | 49 | 40.1 | 37-38.1 | 121-45.8 | 1.2 | 1.5 | 14 | 121 | 12.1 | 0.11 | 0.4 | 0.7 | B | LIVERMORE |
| | | 5 | 2 | 49 | 59.7 | 37-38.2 | 121-46.1 | 0.4 | 1.4 | 9 | 142 | 11.9 | 0.16 | 0.8 | 6.3 | C | LIVERMORE |
| | | 9 | 23 | 55 | 23.7 | 37-37.9 | 121-45.9 | 1.5 | 2.1 | 17 | 120 | 12.1 | 0.07 | 0.2 | 0.4 | B | LIVERMORE |
| | | 9 | 23 | 56 | 44.9 | 37-37.9 | 121-45.8 | 2.8 | 1.5 | 10 | 120 | 11.9 | 0.11 | 0.6 | 8.3 | C | LIVERMORE |
| | | 11 | 9 | 46 | 2.7 | 37-37.8 | 121-45.9 | 0.1 | 1.9 | 13 | 118 | 12.0 | 0.09 | 0.3 | 2.4 | C | LIVERMORE |
| | | 11 | 10 | 6 | 1.8 | 37-37.8 | 121-46.1 | 0.0 | 1.3 | 10 | 117 | 12.2 | 0.12 | 0.5 | 4.5 | C | LIVERMORE |
| | OCT | 7 | 20 | 26 | 15.3 | 37-36.4 | 121-47.2 | 3.9 | 1.3 | 8 | 113 | 12.1 | 0.02 | 0.1 | 0.3 | B | LA COSTA VALLEY |
| | | 19 | 1 | 3 | 22.0 | 37-37.7 | 121-55.0 | 1.5 | 1.6 | 11 | 76 | 3.5 | 0.07 | 0.3 | 0.5 | A | DUBLIN |
| | NOV | 4 | 14 | 20 | 46.5 | 37-37.9 | 121-46.0 | 1.4 | 1.7 | 10 | 119 | 12.1 | 0.08 | 0.4 | 0.7 | B | LIVERMORE |
| | | 28 | 0 | 42 | 17.0 | 37-35.1 | 121-50.4 | 9.0 | 1.3 | 8 | 111 | 7.6 | 0.25 | 1.8 | 2.3 | B | LA COSTA VALLEY |
| 1978 | APR | 4 | 13 | 59 | 2.9 | 37-38.5 | 121-49.5 | 4.0 | 1.1 | 13 | 78 | 9.8 | 0.15 | 0.6 | 1.2 | B | LIVERMORE |
| 1979 | JAN | 28 | 7 | 59 | 55.7 | 37-40.1 | 121-47.6 | 6.6 | 1.4 | 14 | 91 | 7.7 | 0.08 | 0.4 | 0.9 | B | LIVERMORE |
| | FEB | 15 | 10 | 45 | 45.9 | 37-37.6 | 121-48.4 | 1.2 | 1.7 | 14 | 76 | 11.8 | 0.13 | 0.4 | 0.8 | B | LIVERMORE |
| | APR | 2 | 15 | 29 | 53.5 | 37-35.3 | 121-50.1 | 5.0 | 2.0 | 26 | 59 | 8.0 | 0.09 | 0.2 | 0.5 | B | LA COSTA VALLEY |
| | AUG | 6 | 18 | 41 | 23.3 | 37-38.1 | 121-50.7 | 10.3 | 2.0 | 18 | 95 | 9.8 | 0.06 | 0.2 | 0.2 | B | LIVERMORE |
| | SEP | 28 | 4 | 4 | 38.4 | 37-36.0 | 121-49.3 | 2.2 | 0.9 | 10 | 81 | 9.8 | 0.06 | 0.3 | 0.6 | B | LA COSTA VALLEY |
| | OCT | 29 | 20 | 55 | 58.8 | 37-38.5 | 121-53.2 | 9.6 | 1.3 | 19 | 79 | 6.3 | 0.06 | 0.2 | 0.3 | A | DUBLIN |

References

Aki, K. and Lee, W. H. K., 1976, Determination of Three-Dimensional Velocity Anomalies under a seismic array using first P arrival times from local Earthquakes, 1. A Homogeneous Initial Model, Journal of Geophysical Research, v. 81, no. 23, pp. 4381-4399.

Bolt, B. A. and Miller, R. D. 1975, Catalog of earthquakes in northern California and adjacent areas. Berkeley Seismographic Station, University of California, Berkeley California, 567 p.

Bonilla, M. G., Lienkaemper, J. J., and Tinsley, J. C., 1980, Surface faulting near Livermore, California associated with the January 1980 earthquakes: U.S. Geological Survey Open-File Report 80-523, 32 p.

Bufe, C. G., Lester, F. W. Meagher, K. L. and Wesson, R. L. 1975, Catalog of earthquakes along the San Andreas fault system in central California, April-June, 1973: U.S. Geological Survey Open-File Report 75-125, 44 p.

Byerly, P., 1939, Near Earthquakes in central California, BSSA, v. 29, pp. 427-462.

California Department of Water Resources, 1964, Crustal Strain and Fault Movement Investigation, Faults and Earthquake Epicenters in California: Bulletin 116-2, 95 p.

Crosson, R. S., Crustal Structure Modeling of Earthquake Data, 1. Simultaenous Least Squares Estimation of Hypocenter and Velocity Parameters, Journal of Geophysical Research, v. 81, pp. 3036-3046.

Earth Science Associates, 1979, Advisory Committee on Reactor Safeguards, Meeting of GETR Subcommittee, November 14, 1979, Presentation by Earth Science Associates: Palo Alto, California. unpaginated.

Ellsworth, W. L., Bear Valley, California, Earthquake Sequence of February-March 1972, Seismological Society of America Bulletin, v. 65, pp. 483-506.

Ellsworth, W. L., and Moths, B. 1978 (i.e., 1979), Seismic structure of the San Andreas fault zone near Dry Lake, California (abs.): Earthquake Notes, v. 49, no. 4, p. 99.

Hall, C. A., Jr., 1958, Geology and Palentology of the Pleasanton area, Alameda and Centra Costa counties, California: Univ. California Pubs. Geol. Sci. Bull. v. 34, no. 1, Map 1, scale 1:39,000.

Herd, D. G., 1977, Geologic Map of the Las Positas, Greenville, and Verona faults, Eastern Alameda County, California: U.S. Geological Survey Open-File Report 77-689, 1 sheet, scale 1:24,000; 25 p. text.

Herd, D. G., 1979, Neotectonic framework of central coastal California and its implications to microzonation of the San Francisco Bay region, _in_, Brabb, E. E., ed., Progress on seismic zonation in the San Francisco Bay region: U.S. Geological Survey Circular 807, p. 3-12.

Lawson, A. C., 1908, Report of the State EArthquake Investigation Commission. A. C. Lawson Chairman, Volume 1, Part 1. Published by the Carnegie Institution of Washington, Washington D. C.

Lee, W. H. K., Eaton, M. S. and Brabb, E. E. 1971, The Earthquake Sequence near Danville, California, 1970, Seismological Society of America Bulletin, v. 61, pp. 1771-1794.

Lee, W. H. K., Roller, J. C. Bauer, P. G. and Johnson, J. D. 1972a, Catalog of earthquakes along the San Andreas fault system in central California for the year 1969: U.S. Geological Survey Open-File Report, 49 p.

Lee, W. H. K., Roller, J. C., Meagher, K. L. and Bennett, R. E. 1972b, Catalog of earthquakes along the San Andreas fault system in central California for the year 1970: U.S. Geological Survey Open-File Report 73 p.

Lee, W. H. K., Meagher, K. L., Bennett, R. E. and Matamoros, E. E. 1972c, Catalog of earthquakes along the San Andreas fault system in central California for the year 1971: U.S. Geological Survey Open-File Report, 62 p.

Lester, R. W., Kirkman, S. L. and Meagher, K. L. 1976b, Catalog of earthquakes along the San Andreas fault system in central California. October-December 1973: U.S. Geological Survey Open-File Report 76-732, 37 p.

Lester, F. W., and Meagher, K. L. 1978, Catalog of earthquakes along the San Andreas fault system in central California, for the year 1974: U.S. Geological Survey Open-File Report 78-1010, 89 p.

Lester, F. W., Meagher, K. L. and Wesson, R. L. 1976a, Catalog of earthquakes along the San Andreas fault system in central California, July-September, 1973: U.S. Geological Survey Open-File Report 76-169, 38 p.

Mayer-Rosa, Dieter, 1973, Traveltime anomalies and distribution of earthquakes along the Calaveras fault zone, California: Seismological Society of America Bulletin, v. 63, p. 713-729.

McHugh, C. A., and Lester, F. W. (1978a), Catalog of earthquakes along the San Andreas fault system in central California, for the year 1975: U.S. Geological Survey Open-File Report 79-1138, 91 p.

McHugh, C. A., and Lester, F. W. 1978b, Catalog of earthquakes along the San Andreas fault system in central California, for the year 1976: U.S. Geological Survey Open-File Report 78-1051, 91 p.

Nason, R. D., 1971, Investigation of Fault Creep Slippage in Northern and Central California. Ph.D. thesis, University of California at San Diego. University Microfilms No. 72-12, 246-746 p.

Savage, J. E., and Burford, R. O., 1973, Geodetic Determination of Relative Plate Motion in central California, Journal of Geophysical Research, v. 78, pp. 832-845.

Stewart, S. W., 1968, Preliminary comparison of seismic traveltimes and inferred crustal structure adjacent to the San Andreas fault in the Diablo and Gabilan Ranges of central California, in Dickinson, W. R., and Grantz, A., eds., Proceedings of Conference on Geologic Problems of San Andreas Fault System: Stanford University Publications in Geological Sciences, v. 11, p. 218-230.

Thatcher, W., 1975, Strain Accumulation on the Northern San Andreas Fault Zone since 1906, Journal of Geophysical Research, v. 80, pp. 4873-4880.

Toppozada, T. R., Real, C. R., Bezore, S. P. and Parke D. L. 1979, Compilation of Pre-1900 California Earthquake History. Annual Tech. Rept. for FY 1978 to 1979, for period February 10, 1978 to February 9, 1979. California Division of Mines and Geology, Open-File Report 79-6 SAC., 271 p.

Wesson, R. L., Bennett, R. E. and Meagher, K. L. 1972a, Catalog of earthquakes along the San Andreas fault system in central California, January-March, 1972: U.S. Geological Survey Open-File Report, 60 p.

Wesson, R. L., Bennett, R. E. and Lester, F. W. 1972b, Catalog of earthquakes along the San Andreas fault system in central California, April-June, 1972: U.S. Geological Survey Open-File Report, 42 p.

Wesson, R. L., Meagher, K. L. and Lester, F. W. 1973a, Catalog of earthquakes along the San Andreas fault system in central California, July-September, 1972: U.S. Geological Survey Open-File Report, 49 p.

Wesson, R. L., Lester, F. W. and Meagher, K. L. 1974a, Catalog of earthquakes along the San Andreas fault system in central California, October-December, 1972: U.S. Geological Survey Open-File Report, 46 p.

Wesson, R. L., Lester, F. W. and Meagher, K. L. 1974b, Catalog of earthquakes along the San Andreas fault system in central California, January-March, 1973: U.S. Geological Survey Open File Report, 46 p.

# Figure Captions

Figure 1. Location map for the Livermore Valley, California study area. Triangles denote seismograph stations used to locate earthquakes. Star marks location of San Ramon shotpoint.

Figure 2. Index map for place names and faults mentioned in text.

Figure 3. Seismicity of the Livermore Valley, California region for the years 1969-1979. Earthquake epicenters (octagons) are scaled with magnitude. Candidate faults discussed in text which also appears in Figure 2 are shown.

Figure 4. Representative lower hemisphere focal mechanism solutions for earthquakes in the study area. Compressional quadrant is shaded.

Figure 5. P and T axes of focal mechanisms of earthquakes in the Livermore Valley, California region.

Figure 6. Well-located aftershocks of the January 24, 1980 Livermore earthquake ($M_L$ 5.8).

Figure 7. Seismicity near the General Electrict Test Reactor (GETR) for the years 1969-1979. Earthquake symbols plotted are focal depth in kilometers (0-1 km: 0, 1-2 km: 1, ..., 10-11 km: A, etc.). Points labeled a and a' identify end points of cross section in Figure 9.

Figure 8. Lower hemisphere focal mechanism solutions for earthquakes shown in Figure 8. Compressional quadrant is shaded.

Figure 9. Longitudinal cross-section of seismicity along the dip direction of the Verona fault. Only events within 4 km of section line are plotted. Symbols plotted are the same as those shown in Figure 7. Dashed line represents position of the Verona fault for a $45^{\circ}$ dip to the northeast.

Figure 1

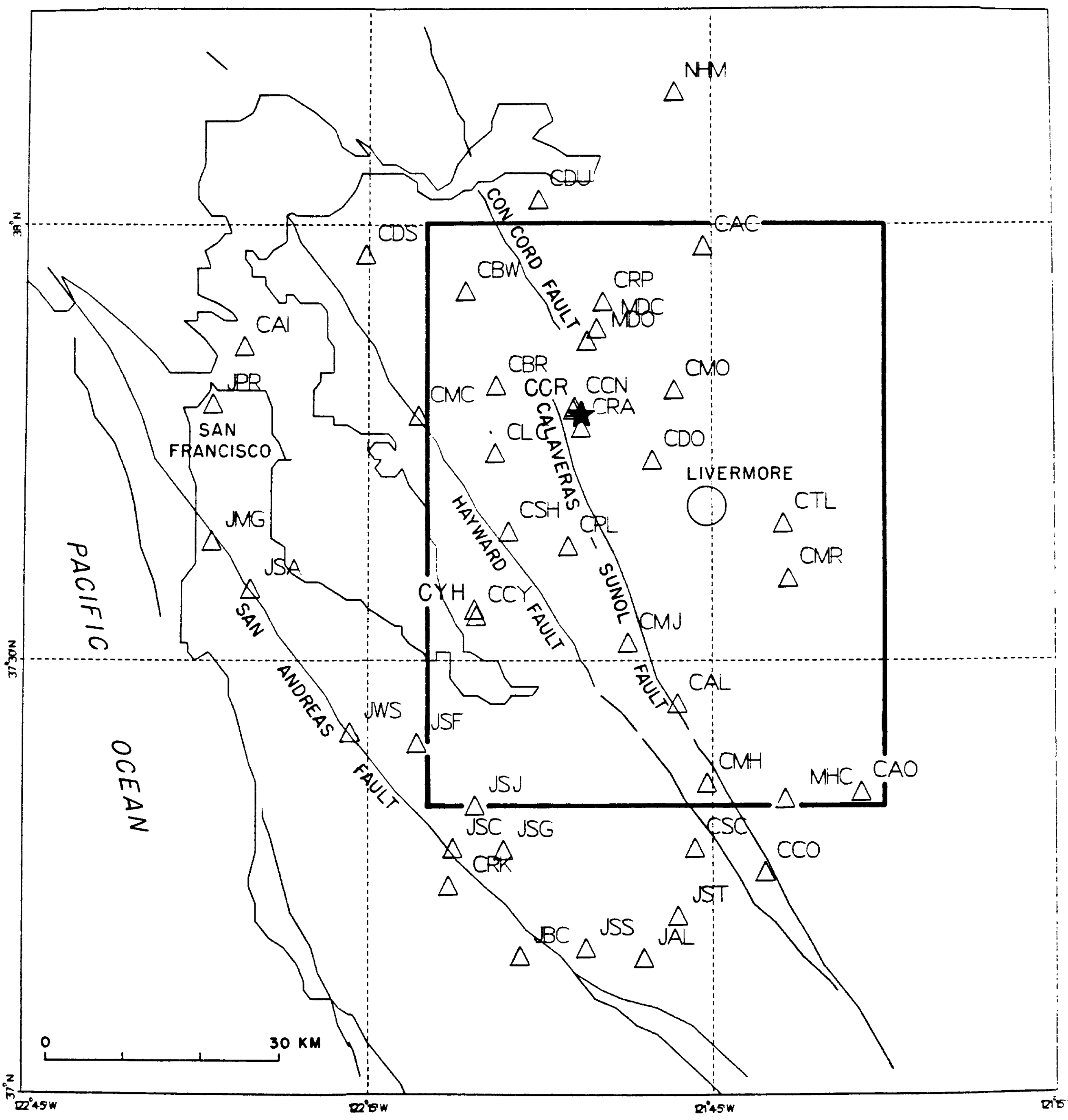
NHM
CDU
CAC
CDS
CBW
CON CORD FAULT
CRP
MDC
MDO
CAI
CBR
CCR
CCN
CMO
JPR
CMC
CRA
SAN FRANCISCO
CLC
CALAVERAS
CDO
LIVERMORE
CTL
JMG
CSH
CPL
HAYWARD FAULT
CMR
JSA
CYH
CCY
SUNOL
CMJ
PACIFIC
SAN
FAULT
CAL
ANDREAS
JWS
JSF
OCEAN
CMH
MHC
CAO
FAULT
JSJ
JSC
JSG
CSC
CCO
CRK
JST
JBC
JSS
JAL
0
30 KM
38°N
37°30N
37°N
122°45W
122°15W
121°45W
121°15W

Figure 2

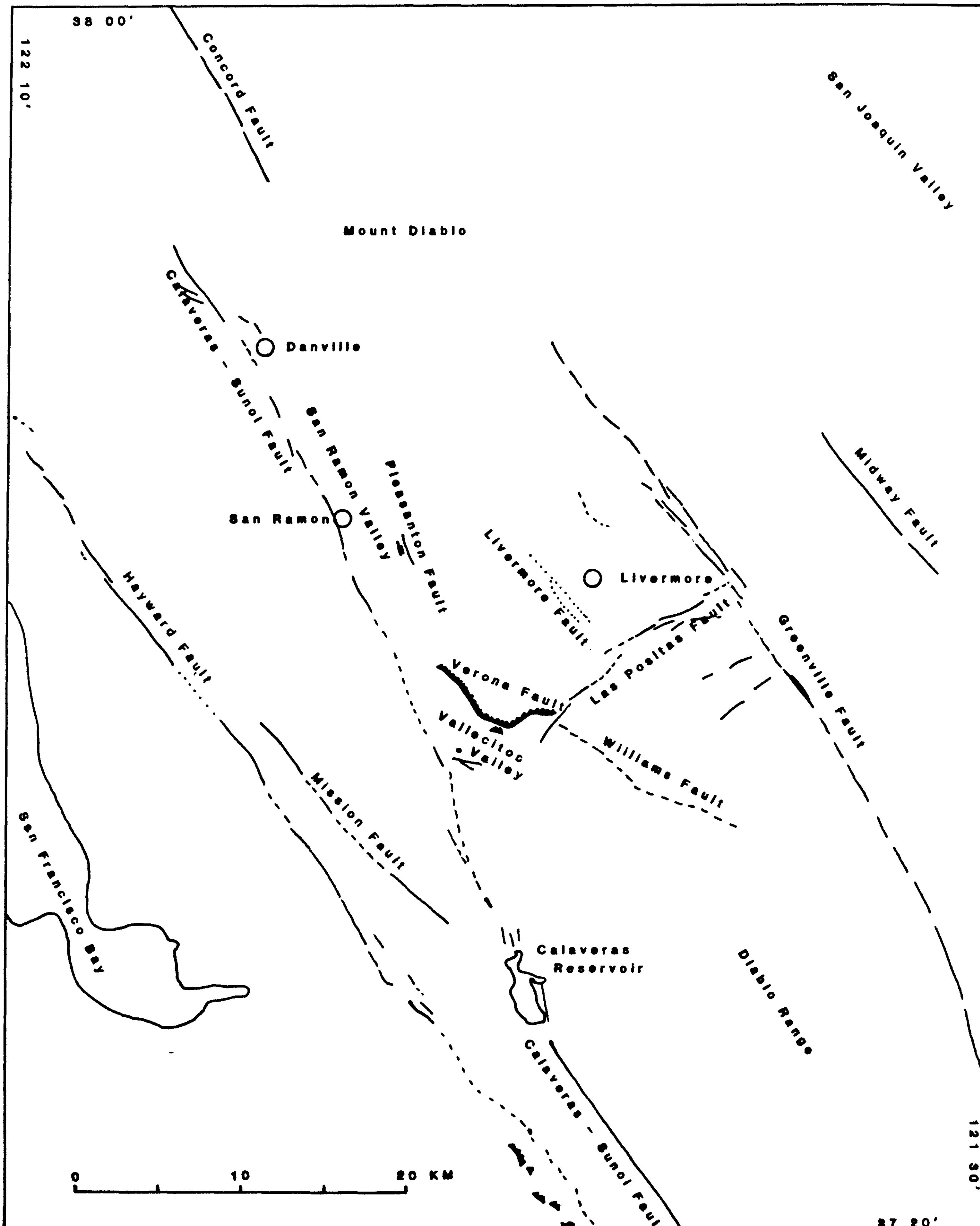

38 00'
122 10'
Concord Fault
San Joaquin Valley
Mount Diablo
Calaveras - Sunol Fault
Danville
San Ramon Valley
Pleasanton Fault
San Ramon
Midway Fault
Livermore Fault
Livermore
Hayward Fault
Greenville Fault
Las Positas Fault
Verona Fault
Vallecitos Valley
Williams Fault
Mission Fault
San Francisco Bay
Calaveras Reservoir
Diablo Range
Calaveras - Sunol Fault
0
10
20 KM
121 30'
37 20'

# LIVERMORE REGION STUDY AREA

Figure 3

1969 – 1979

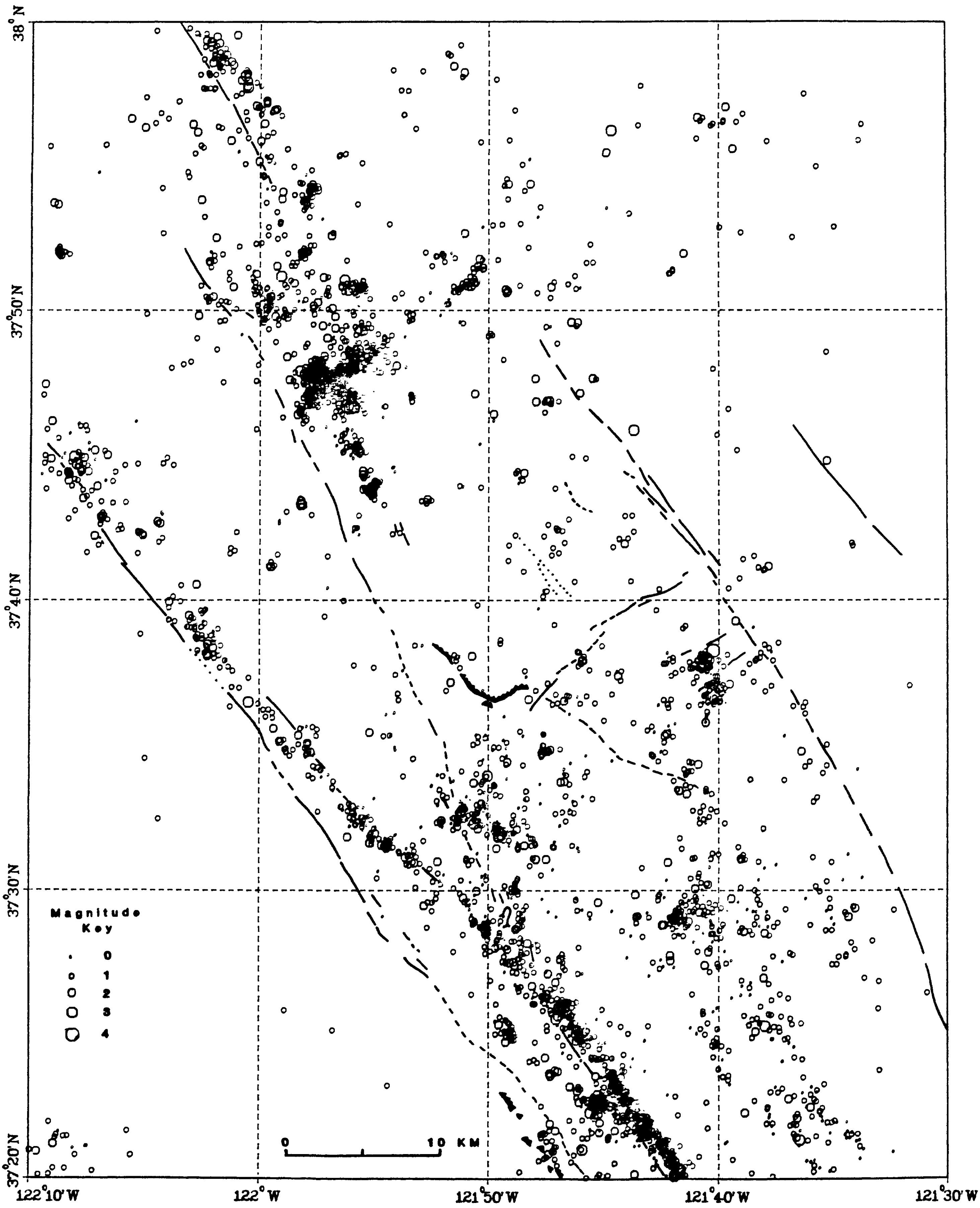

Figure 4

LIVERMORE REGION STUDY AREA

SELECTED FOCAL MECHANISM SOLUTIONS

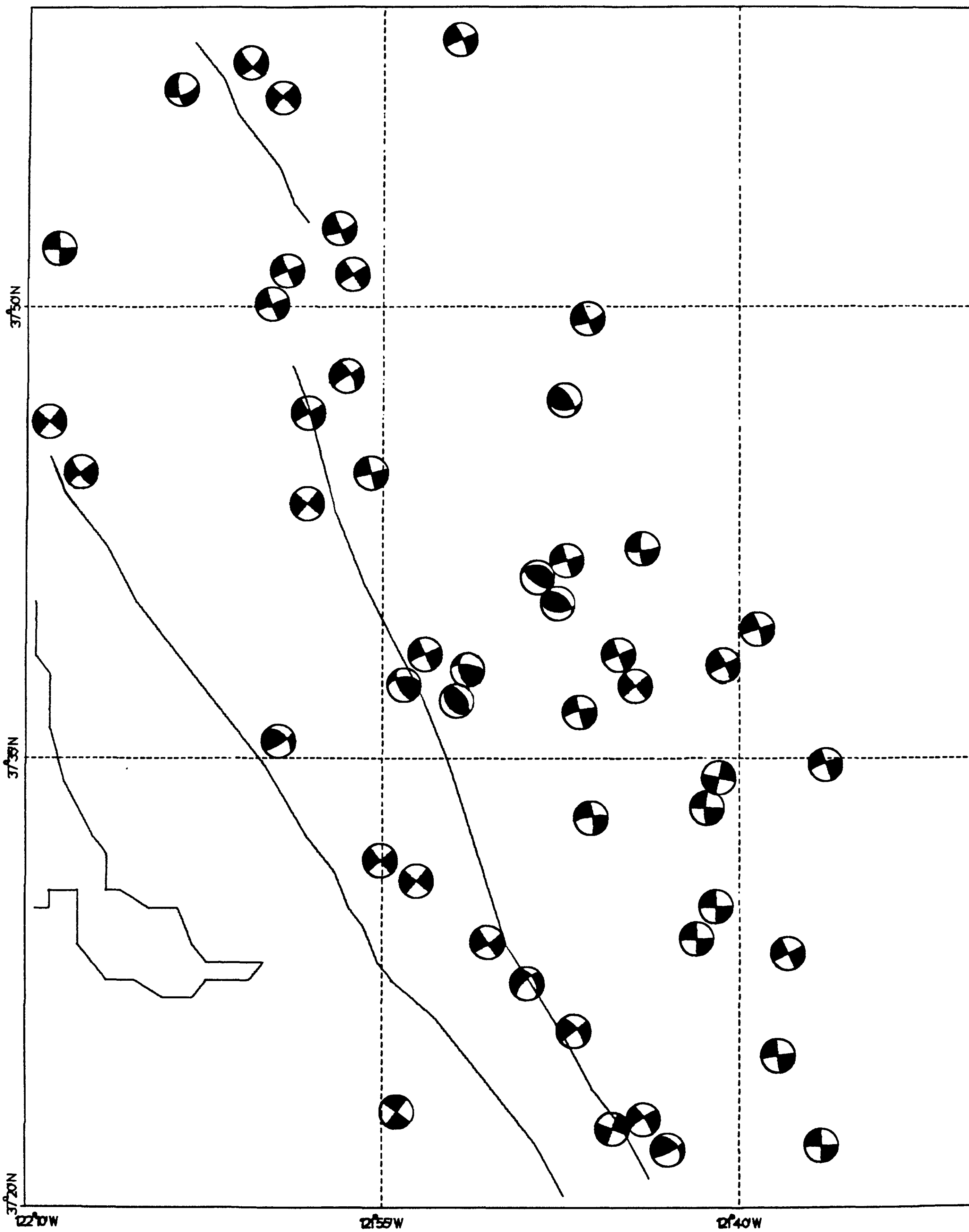

Figure 5 

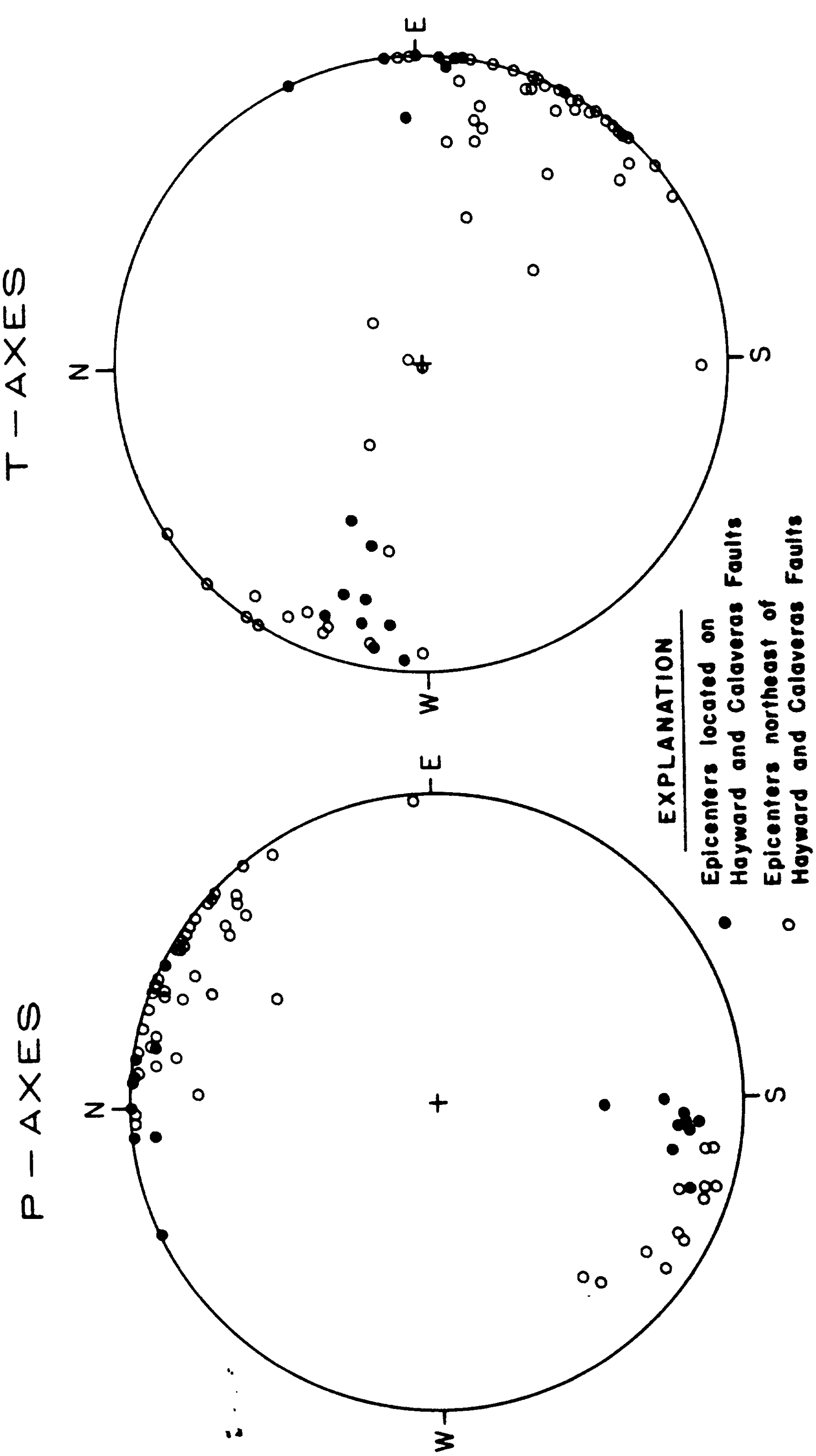
P — AXES
T — AXES
N
E
S
W
EXPLANATION
Epicenters located on Hayward and Calaveras Faults
Epicenters northeast of Hayward and Calaveras Faults

Figure 6



# LIVERMORE VALLEY EARTHQUAKES

## JAN 24 – FEB 26 1980

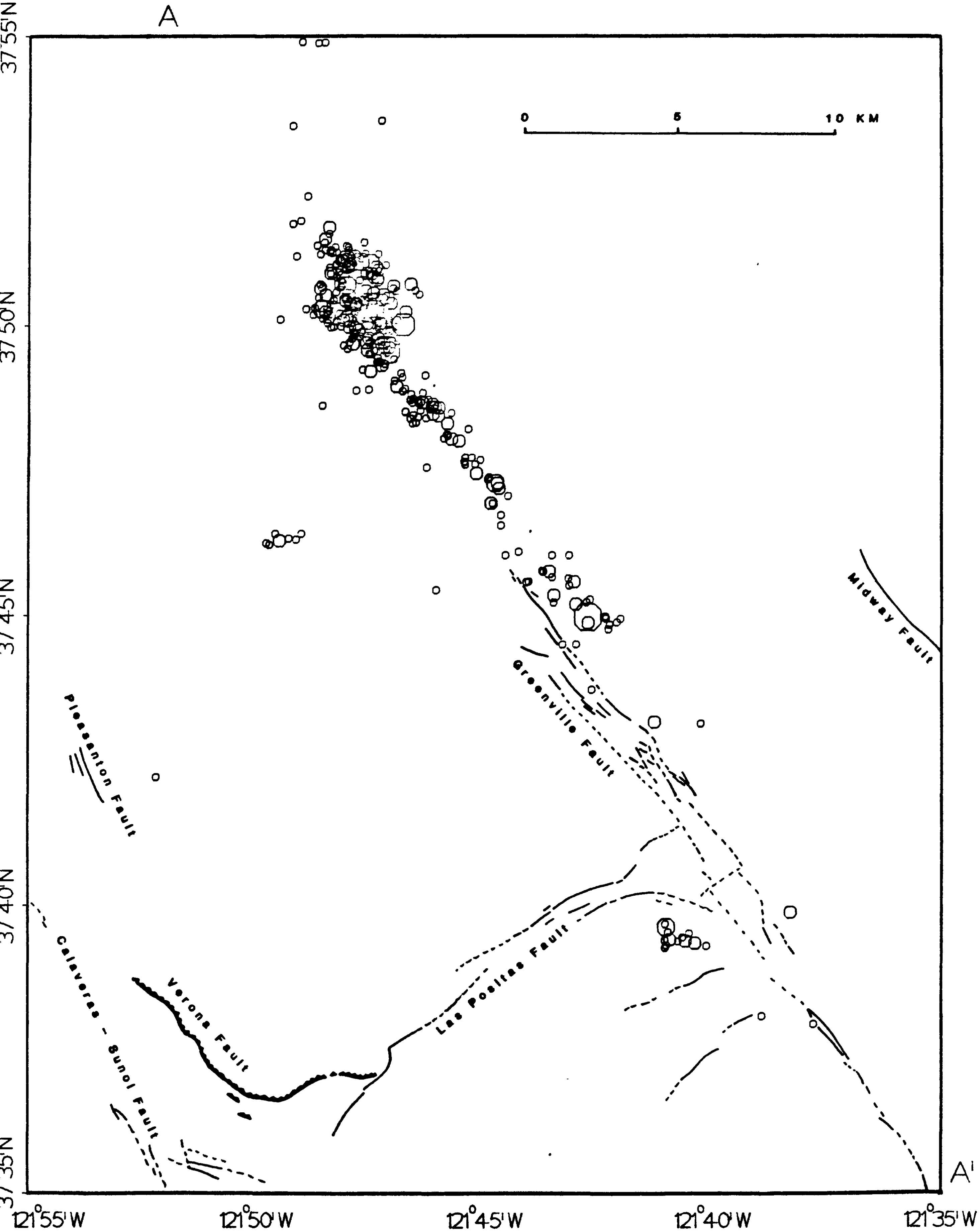

Figure 7

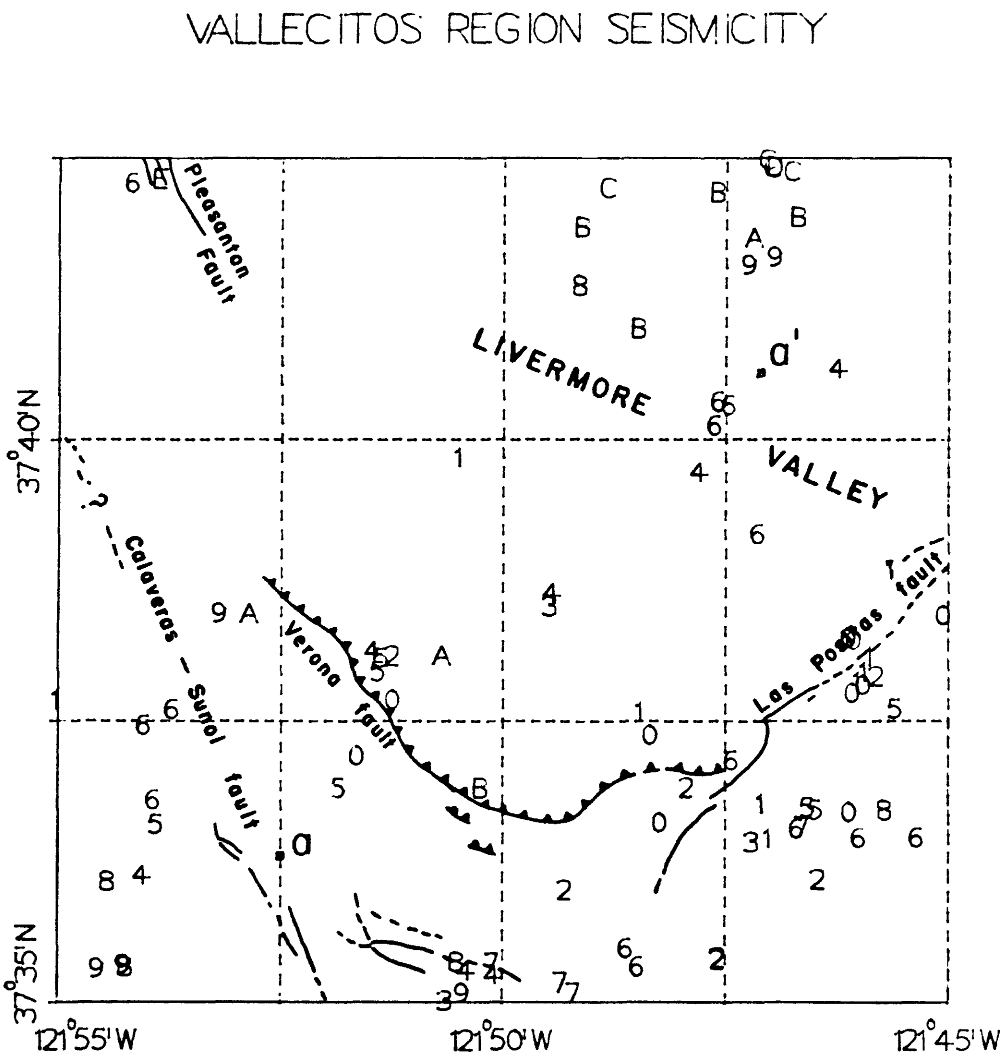
VALLECITOS REGION SEISMICITY
Pleasanton Fault
LIVERMORE
VALLEY
Calaveras - Sunol fault
Verona fault
Las Positas fault
37°40'N
37°35'N
121°55'W
121°50'W
121°45'W

Figure 8

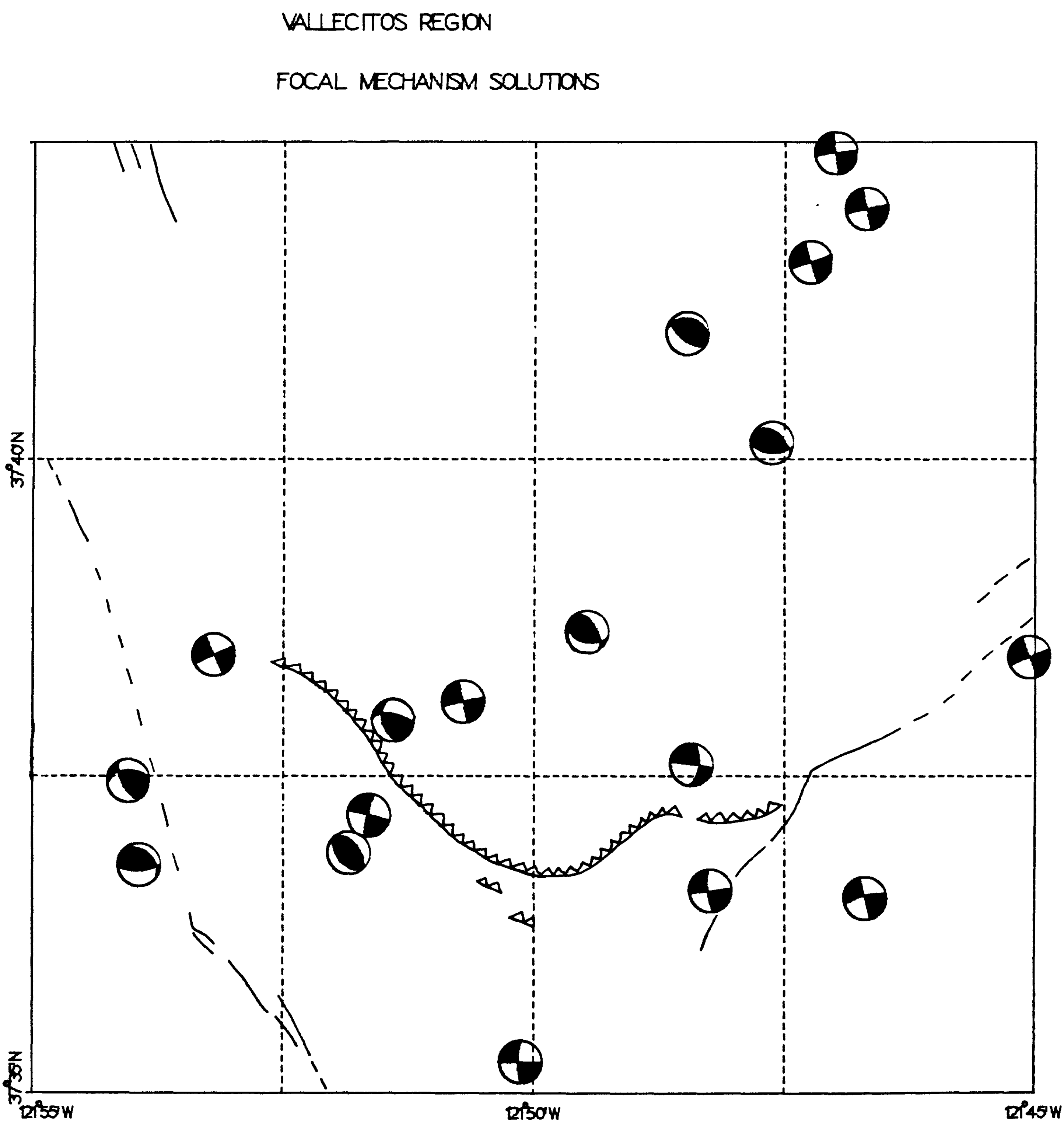
VALLECITOS REGION
FOCAL MECHANISM SOLUTIONS
37°40'N
37°35'N
121°55'W
121°50'W
121°45'W

Figure 9